

# Effect of the Initial Crystallographic Texture on Microstructure and Mechanical Properties of Mg-3Al-1Zn Sheet Alloy Processed by Half Channel Angular Extrusion (HCAE)

Kyungjin Kim<sup>1</sup> and Jonghun Yoon<sup>2#</sup>

<sup>1</sup> School of Mechanical and Automotive Engineering, Kyungil University, 50, Gamsil-gil, Hayang-eup, Gyeongsan-si, Gyeongsangbuk-do, 712-701, South Korea

<sup>2</sup> Department of Mechanical Engineering, Hanyang University, 55, Hanyangdaehak-ro, Sangnok-gu, Ansan-si, Gyeonggi-do, 426-791, South Korea

# Corresponding Author / E-mail: yooncsmd@gmail.com, TEL: +82-31-400-5259, FAX: +82-31-400-4709

KEYWORDS: Severe plastic deformation, Texture, Mg-3Al-1Zn sheet alloy, Half Channel Angular Extrusion (HCAE)

*In this work, half channel angular extrusion, a recently developed severe plastic deformation (SPD) process, applied to AZ31 Mg alloy. Effects of the initial microstructure of AZ31 alloy on the microstructural development such as the grain refinement and texture evolution during the half channel angular extrusion (HCAE) has been studied. It was found that the grains of the AZ31 alloys can be refined remarkably by single pass of HCAE than other SPD techniques and not only the grain refinement but also the deformation induced textures result in a noticeable enhancement of mechanical properties.*

Manuscript received: August 14, 2014 / Revised: February 24, 2015 / Accepted: February 24, 2015

## 1. Introduction

Magnesium (Mg) alloys have been extensively researched in the transportation and electronic industries since they show high specific strength, high vibration absorption, and thermal management.<sup>1,2</sup> However, there are several limitations in the physical applications for structural components in automobiles due to poor formability,<sup>3-5</sup> corrosion issues, and strength differential effect in the plastic flows between tension and compression.<sup>3,6,7</sup>

For bulk processing techniques to fabricate ultrafine-grained materials, severe plastic deformation (SPD) methods such as high-pressure torsion (HPT),<sup>8</sup> equal channel angular extrusion (ECAE),<sup>9-12</sup> multi-axial forging(MAF),<sup>13,14</sup> and accumulative roll-bonding (ARB)<sup>15</sup> have been proposed as effective ways of enhancement in ductility and grain refinement. Kim et al.<sup>16</sup> proposed the half channel angular extrusion (HCAE) to increase the efficiency in SPD by integrating both ECAE and a conventional forward extrusion process, which maximizes the applied plastic strain to the materials with a small number of repetitive processes.

There also have been extensive researches for increasing the strength and ductility of Mg alloys by refining the microstructure via

severe plastic deformation (SPD). Mabuchi et al.<sup>17</sup> demonstrated that a very fine-grained AZ91 magnesium alloy processed by equal channel angular extrusion showed low-temperature superplasticity. Yamashita et al.<sup>18</sup> conducted equal channel angular pressing (ECAP) to evaluate the potential for improving the mechanical properties of Mg alloys, and Mukai et al.<sup>19</sup> reported that the elongation-to-failure of the ECAE/annealed alloy increased up to 50%. Agnew et al.<sup>20</sup> showed a wide range of deformation-induced textures during the ECAE of magnesium alloys. Xia et al.<sup>21</sup> conducted ECAP up to 8 passes in which the initial coarse-grained structure was transformed into a submicrometer-grained microstructure. Suwas et al.<sup>22</sup> showed that the improved cold formability was attributed to the initial non-basal texture and grain refinement introduced by ECAE.

In general, ECAE process with Mg alloys has been carried out at temperatures around 473K or above since it is difficult to accomplish the several passes of ECAE at room temperature successfully without fine cracks in the specimens. It results in undesirable decreases in the mechanical properties of the ECAE-processed specimen such as the yield and ultimate strengths since the elevated forming temperature induces the dynamic recrystallization (DRX) of the Mg alloys, which develops strain-free grains with low level of dislocation density in the

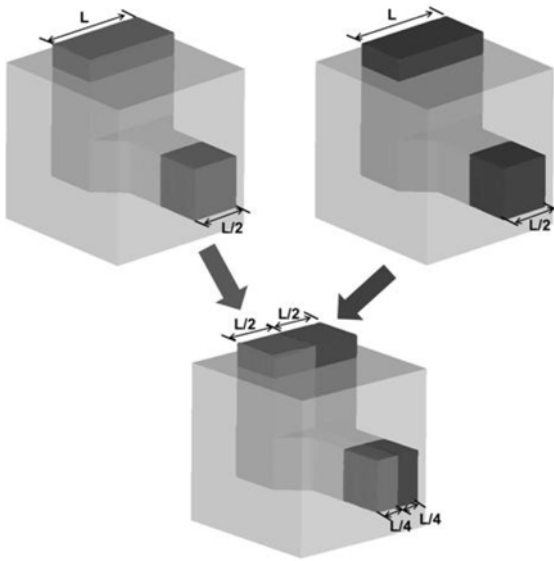


Fig. 1 Schematic diagrams of HCAE process<sup>16</sup>

whole grain structure.<sup>23,24</sup> Therefore, it is substantial to correlate the enhancement of formability and mechanical strength in the ECAE-processed materials by microstructural development with the DRX and texture effects in the Mg alloys, systematically. Foley et al.<sup>25</sup> demonstrated that it was effective to decrease the processing temperature in SPD process for grain refinement with AZ31B Mg alloy. Tang et al.<sup>23</sup> investigated the effects of the initial texture on the yield strength and ductility of the ECAEed Mg-Zn-Y-Zr alloy. Al-Maharbi et al.<sup>24</sup> reported that the starting texture had strong influences on the mechanical properties of Mg alloy after ECAE/ECAP such as flow anisotropy and tension/compression asymmetry. They also concluded that it was possible to control the level of mechanical anisotropy in the ECAE-processed samples and obtain strongly or weakly anisotropic mechanical response in Mg alloys by proper selection of the starting texture and ECAE route.

In this work, effects of the initial crystallographic texture of Mg-3Al-1Zn sheet alloy on the microstructural development in terms of the grain refinement and texture evolution during the half channel angular extrusion (HCAE) has been studied. Microstructures and mechanical properties of Mg-3Al-1Zn sheet alloy were evaluated with respect to the starting textures. Microstructural characterization with HCAE-processed Mg-3Al-1Zn sheet alloys has been investigated by optical microscopy (OM) and orientation imaging microscopy (OIM) analysis using electron backscattered diffraction (EBSD) technique and tensile tests were carried out to examine the mechanical properties of the HCAE-processed specimens at the room temperature with the strain rate of 0.001/sec.

## 2. Experimental Procedures

Kim et al.<sup>16</sup> have proposed a SPD process for applying more severe plastic deformation to the billet with a small number of repetitive processes by integrating an equal channel angular extrusion and a conventional forward extrusion process as shown in Fig. 1. There is

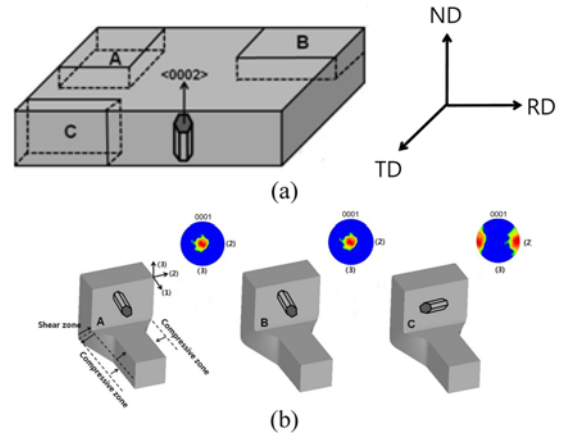


Fig. 2 Initial specimens for HCAE experiments with Mg-3Al-1Zn rolled sheet alloy: (a) three kinds of specimens with respect to starting texture; (b) HCAE-processed billets with specimen-A, B, and C

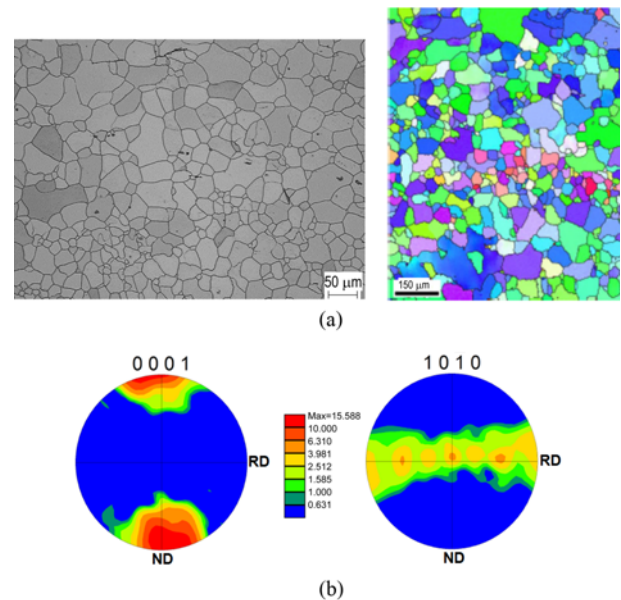


Fig. 3 Initial microstructure of Mg-3Al-1Zn rolled sheet alloy: (a) OM and EBSD observations; (b) initial texture

area reduction in the exit channel to a 2:1 since the width of the exit channel is gradually reduced to half of that of the entry channel. The HCAE process tends to induce severe plastic deformation with shear which is employed by the intersecting angle ( $\Phi=90^\circ$ ,  $\Psi=10^\circ$ )<sup>16</sup> between the entry and exit channels and compressive plastic deformation to the initial billet. It does not only induce additional plastic deformation about 50% compared to the conventional ECAP,<sup>16</sup> but also enhance the process efficiency because two HCAE-processed billets from the first pass are applied to the second pass of the HCAE, simultaneously, by combining them into one full billet as shown in Fig. 1.

The initial specimens for the HCAE process have the dimension of  $25 \times 50 \times 70 \text{ mm}^3$ , which are classified into three kinds of specimen-A, B, and C with respect to texture orientation. The specimen-A, B, and C are prepared by machining them from the Mg-3Al-1Zn rolled sheet alloy

(Mg-3%Al-1%Zn) with the thickness of 50 mm as depicted in Fig. 2(a), which are subjected to compression along the rolling (RD), transverse (TD), and normal (ND) directions, respectively, during the HCAE process as shown in Fig. 2(b). Fig. 3 shows the microstructural characteristics of the Mg-3Al-1Zn rolled sheet alloy in which it has the average grain size of 72.7  $\mu\text{m}$ . It is apparent that the most of grains are equiaxed and the distribution of grain sizes in the initial specimen for HCAE are quite non-uniform, as it has small grains of less than 10  $\mu\text{m}$  and larger ones than 100  $\mu\text{m}$ . The starting material for the HCAE process has strong (0001) textures parallel to the ND since the initial material was fabricated from rolling process, which makes the specimens for the HCAE process have different textures from each other according to the orientation of the machined direction of the rolled sheet.

To guarantee appropriate formability of the test specimen during the HCAE process, the target temperature was fixed with 523K, which was maintained with ten heating rods inserted to upper and lower dies, separately. Fig. 4 demonstrated the initial die-set for the HCAE process including hydraulic cylinders which are installed at both sides in the die-set against when the test specimen is stuck between upper and lower dies as shown in Fig. 4(b). The plunger travels downward in the 450-ton press shop with a crosshead speed of 5mm/sec when the target temperature of the die-set reaches 523K.

In order to compare the microstructure of HCAE-processed with the as-received Mg-3Al-1Zn sheet alloys depending on the starting texture such as specimen-A, B, and C, optical microscopy (OM) and EBSD experiments installed in a field emission scanning electron microscope (Hitachi SU6600) were carried out for quantitative analysis. OM specimens are prepared with cold mounting which is made of epoxy resin and hardener with the ratio of 100:12 with curing time of 8 hours at room temperature in case that compressive force during hot mounting is able to induce minor twins. EBSD specimens are prepared with chemo-mechanical polishing using colloidal silica under a pressing force of 17 N for 1 hour after a mechanical polishing with sand paper up to 800 grit and 3  $\mu\text{m}$  diamond pastes to provide a high quality of surface finish.

### 3. Experimental Results

#### 3.1 Microstructure

Three different test specimens-A, B, and C with respect to the initial textures are applied to the proposed HCAE process as shown in Fig. 2(a) at the forming temperature of 523 K. Figs. 5 and 6 show the OM investigations according to the observed planes such as 2-3 and 1-3 as depicted in Fig. 2(b) in the HCAE-processed specimens by applying specimen-A, B, and C. HCAE-processed-A and -B include large fraction of deformed grains surrounded by fine DRX grains. The general features of the microstructures observed on the 1-3 planes in the HCAE-processed-A and B are mixtures of elongated and equiaxed grains. The elongated grains oriented approximately 23° CCW from the 1-axis due to the intersecting angle between the entry and exit channels and compressive deformation during the HCAE process. While the HCAE-processed-C has more uniform grain structure with large fraction of recrystallized fine grains as shown in Figs. 5(c) and 6(c).

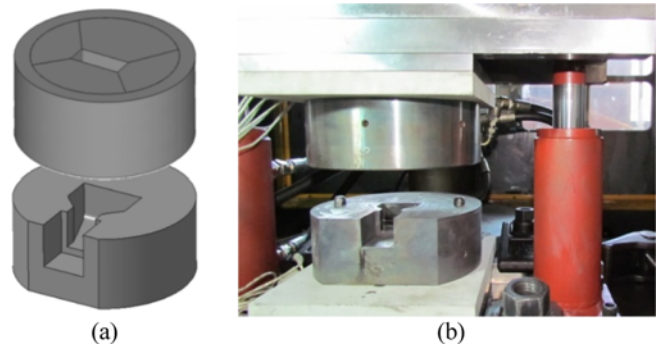


Fig. 4 die-set for HCAE process: (a) schematic design of upper and lower dies; (b) installation of die-set with hydraulic cylinders<sup>16</sup>

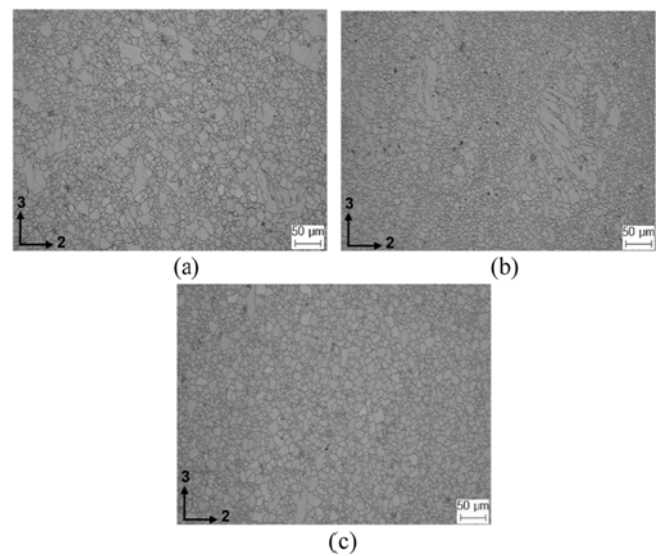


Fig. 5 Microstructures of HCAE-processed specimens in 2-3 plane: (a) HCAE-processed-A; (b) HCAE-processed-B; (c) HCAE-processed-C

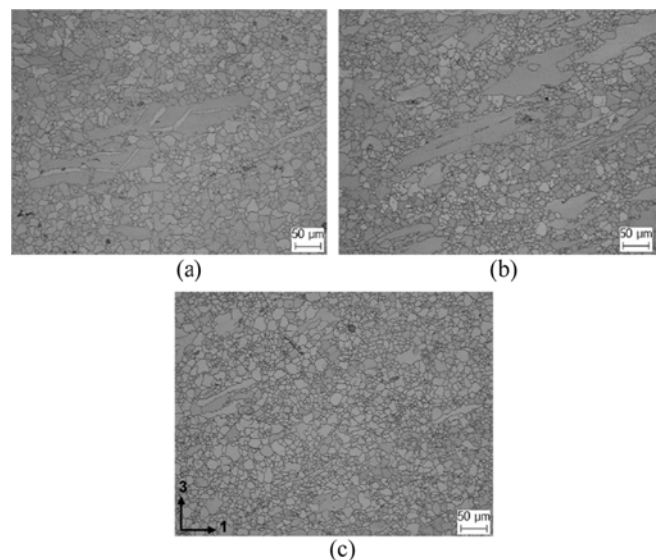


Fig. 6 Microstructures of HCAE-processed specimens in 1-3 plane: (a) HCAE-processed-A; (b) HCAE-processed-B; (c) HCAE-processed-C

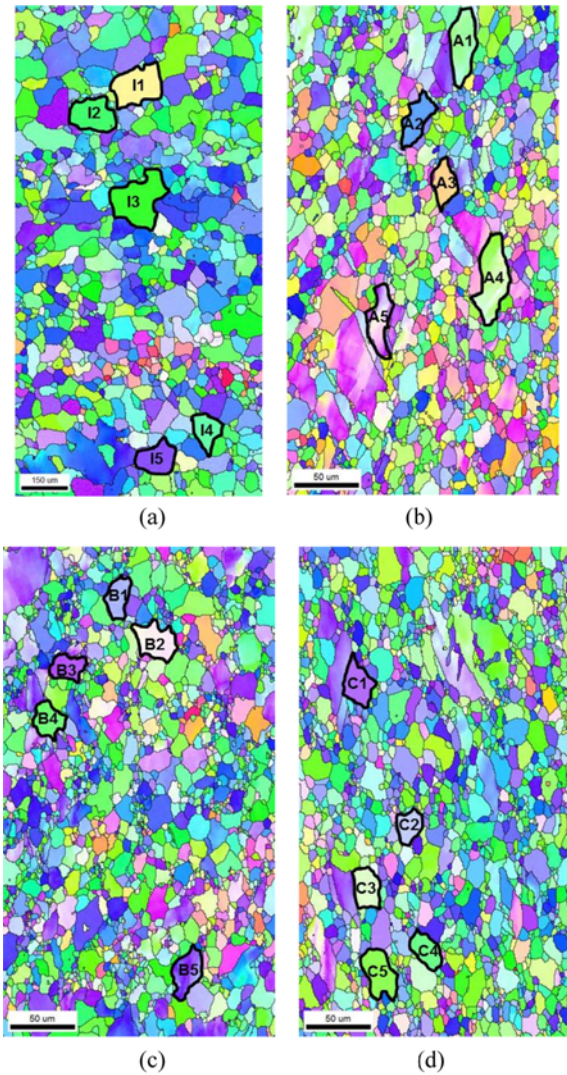


Fig. 7 Grain maps constructed by EBSD results on 2-3 plane: (a) as-received; (b) HCAE-processed-A; (c) HCAE-processed-B; (d) HCAE-processed-C

For quantitative comparisons of grain structures in the HCAE-processed specimens, Fig. 7 demonstrates grain maps constructed by EBSD. The average grain sizes of the HCAE-processed-A, B, and C decreased from 72.7  $\mu\text{m}$  in the starting materials to 13.7, 15.4, and 12.9  $\mu\text{m}$ , respectively, with the standard deviation of 4.5, 4.9, and 4.2  $\mu\text{m}$  in a single pass of HCAE. For comparisons, ECAE can reduce the grain size of Mg alloys from 24.4  $\mu\text{m}$  to 8.4  $\mu\text{m}$  at 548 K and from 45.5 to 26.7  $\mu\text{m}$  at 523 K after eight passes.<sup>26,27</sup> It is concluded that the HCAE-processed-C has been recrystallized more uniformly during the HCAE process. Fig. 8 shows the distributions of misorientation angle along the line with the length of 20  $\mu\text{m}$  in five representative grains which are selected by the grain size over 20 $\mu\text{m}$  for one side of that marked with thick black line in Fig. 7.

It is interesting that the fraction of low angle grain boundaries with the misorientation angle of less than 5° is about 30 % in the as-received and it is not influenced by the HCAE process for the HCAE-processed-A, B for the whole measured domain as shown in Fig. 9. In general, the population at low misorientation angle, 0-5°, is not changed after SPD

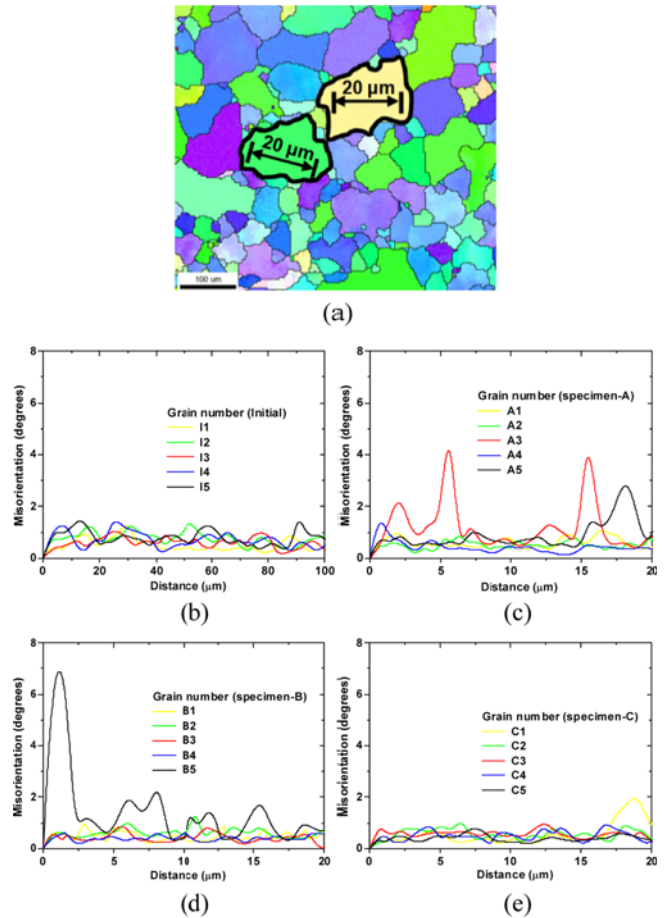


Fig. 8 Distribution of misorientation angle in the representative grains along 20  $\mu\text{m}$ : (a) representative grain; (b) as-received; (c) HCAE-processed-A; (d) HCAE-processed-B; (e) HCAE-processed-C

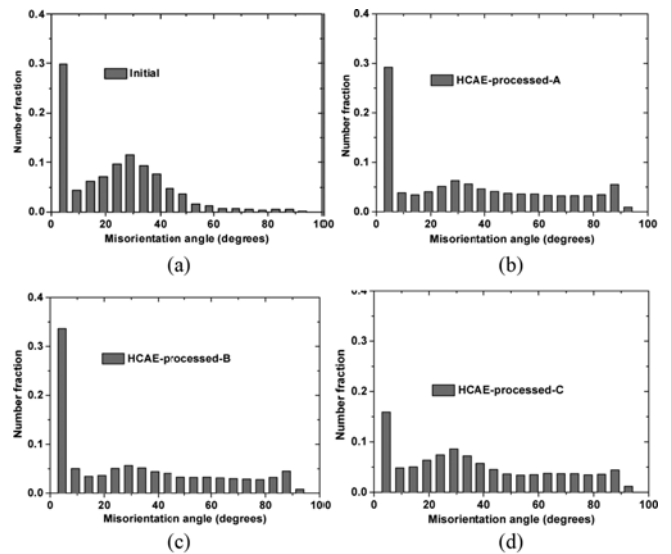


Fig. 9 Distribution of misorientation angle in measured domain: (a) as-received; (b) HCAE-processed-A; (c) HCAE-processed-B; (d) HCAE-processed-C

process due to the strain-induced grain fragmentation that evolved by

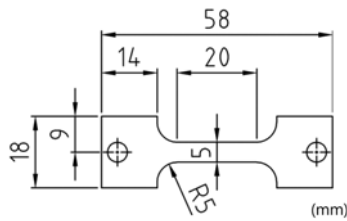


Fig. 10 Dimension of tensile test specimen

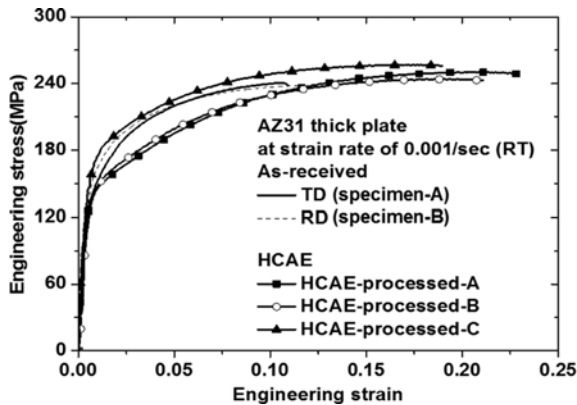


Fig. 11 Comparison of tensile test results with as-received and HCAE-processed at room temperature

the SPD process, in which a fraction of low angle boundaries is always present due to creation of new subgrain boundaries. Interestingly, the populations of misorientation angle in  $10\text{--}40^\circ$  are noticeably diminished and transferred to boundaries with a misorientation angle over  $40^\circ$ , which are most favorable for grain boundary sliding. In addition, the fraction of low angle grain boundaries with the misorientation angle of less than  $5^\circ$  is reduced to 15% in the HCAE-processed-C.

It has been reported that DRX tends to be activated easily when the recovery is slow<sup>24,28</sup> in materials with low stacking fault energy (SFE). Concerning the plastic deformation of Mg alloys at the elevated temperatures, DRX is readily activated when the basal slip is more dominant slip system rather than the other non-basal slip systems such as the prismatic and pyramidal because the basal plane has the lowest SFE of  $32\text{--}36$  (mJ/m<sup>2</sup>).<sup>24,28</sup> Al-Maharbi et al.<sup>24</sup> demonstrated that the volume fraction of recrystallized grains is substantially low when the prismatic slip is the most prevalent in the conventional ECAE process with Mg alloys since activity of prismatic slip acts as a relaxation mechanism, which does not only reduce the amount of internal stress but also decrease the available energy for DRX. Therefore, they presented the highest volume fraction of deformed grains in the processed specimen when applying IA-II specimen<sup>24</sup> which has the same starting texture with the specimen-C in this paper. It is worthy of notice that it produces the most uniform grain structure in the proposed HCAE process even though applying the specimen-C which is able to induce the prismatic slip dominantly. In case of the HCAE-processed-C, dominant prismatic slip does suppress concentration of DRX, which results in large fraction of elongated deformed grains in shear zone of the HCAE process as shown in Fig. 2(b). Then, they tend to experience

Table 1 Comparison of mechanical properties in HCAE-processed

Specimens	Yield strength (YS, MPa)	Ultimate tensile strength (UTS, MPa)	Elongation (EL, %)
RD (as-received)	142	238	12
TD (as-received)	150	239	12
HCAE-processed-A	134	248	23
HCAE-processed-B	136	243	22
HCAE-processed-C	166	257	19

the DRX around the compressive zone of the HCAE process, sequentially, which leads to the uniform grain structure in the HCAE-processed-C compared with HCAE-processed-A and -B.

### 3.2 Mechanical properties of HCAE-processed

Tensile tests were carried out to evaluate the mechanical properties of the HCAE-processed specimens at the room temperature with the strain rate of 0.001/sec. The tensile test specimens of 1 mm thickness are fabricated along 1-axis from the HCAE-processed-A, B, and C as shown in Fig. 10. The tensile axis was always parallel to the 1-axis. Fig. 11 shows the engineering stress - engineering strain curves of the as-received and HCAE-processed of Mg-3Al-1Zn alloy. Mechanical properties including the yield (YS), ultimate tensile strengths (UTS), and elongation (EL) along the transverse (specimen-A) and rolling directions (specimen-B) from the as-received Mg-3Al-1Zn sheet alloy show almost identical result as shown in Fig. 11 since the (0001) basal texture is strongly distributed along the thickness direction of the sheet alloy, which are induced from the manufacturing stage of the rolling process. However, the tensile test along the thickness direction (specimen-C) cannot be presented due to a dimensional restriction since we have utilized the Mg-3Al-1Zn sheet alloy with the thickness of 50 mm.

In Fig. 11, the improvement in the EL with HCAE-processed materials is prominent that the EL of all the HCAE-processed specimens substantially increases about 200% compared with the as-received Mg-3Al-1Zn sheet alloy (Table 1). And there are increases in the YS and UTS of the HCAE-processed-C when applying the specimen-C in the HCAE process, while they decrease about 10 MPa in YS due to the enhancement of the EL with the HCAE-processed-A and B compared with the as-received. It is observed that the EL of the HCAE-processed-C is slightly shorter than of the HCAE-processed-A and B. It is interesting to note that mechanical properties of the HCAE-processed-C are enhanced considerably without YS drop although it experiences the DRX which leads to recrystallized strain-free grains during the HCAE process. Fig. 12 shows (0001) and (1010) pole figure distributions after one pass of the HCAE process with specimen-A, B, and C. The deformation induced textures by the HCAE process are characterized that the majority of basal planes are distributed with tilting angle of  $30^\circ$  from the 3-axis, which deviates from previous report presenting the weak basal textures with inclination angle of  $45^\circ$  from extrusion direction (it is same as 1-axis in this work)<sup>29</sup> and the most strong basal textures are developed in the HCAE-processed-C among three HCAE-processed specimens. This discrepancy can be attributed to the combination of shear and extrusion ratio, which results in the enhancement of YS and UTS of the HCAE-processed-C with increase of the EL, simultaneously.

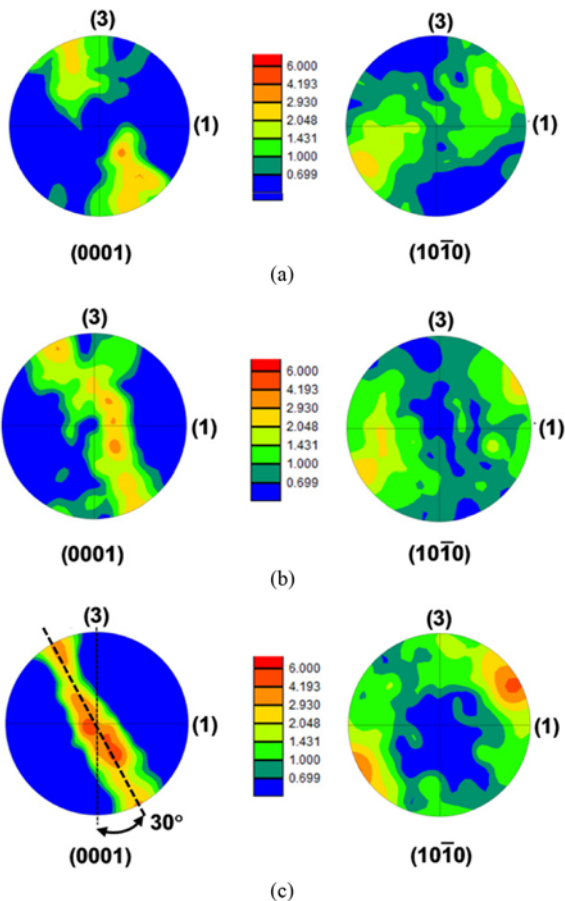


Fig. 12 (0001) and (1010) pole figures after one pass of HCAE process with specimen-A, B, and C

#### 4. Conclusions

Mg-3Al-1Zn rolled sheet alloy is applied to half channel angular extrusion which is integrating both ECAE and a conventional forward extrusion process. The effects of starting textures on the microstructural evolution and change of mechanical properties by HCAE were investigated. The initial specimens for the HCAE process are classified into three kinds of specimen-A, B, and C with respect to texture orientation, which are subjected to compression along the rolling (RD), transverse (TD), and normal (ND) directions during the HCAE process, respectively. The starting material for the HCAE process has strong (0001) textures parallel to the ND since it was fabricated from rolling process. It was found that the microstructures of the AZ31 alloys subjected to the HCAE are refined considerably. HCAE-processed-C has more uniform grain structure with large fraction of recrystallized fine grains than those of HCAE-processed-A and -B. There are increases in the yield strength and ultimate tensile strength of the HCAE-processed-C while HCAE-processed-A and B decreases about 10 MPa in yield strength. And elongation of all the HCAE-processed specimens increases substantially increases about 200% compared with the as-received Mg-3Al-1Zn sheet alloy. In addition, the HCAE-processed-C induced the strong basal textures which are distributed with tilting angle of 30° from the 3-axis. This may results in the enhancement of yield strength and ultimate tensile strength of the

HCAE-processed-C with increase of the elongation, simultaneously.

#### REFERENCES

1. Lou, X. Y., Li, M., Boger, R., Agnew, S. R., and Wagoner, R. H., "Hardening Evolution of AZ31B Mg Sheet," *International Journal of Plasticity*, Vol. 23, No. 1, pp. 44-86, 2007.
2. Khan, A. S., Pandey, A., Gnäupel-Herold, T., and Mishra, R. K., "Mechanical Response and Texture Evolution of AZ31 Alloy at Large Strains for Different Strain Rates and Temperatures," *International Journal of Plasticity*, Vol. 27, No. 5, pp. 688-706, 2011.
3. Yoon, J., Cazacu, O., and Mishra, R. K., "Constitutive Modeling of AZ31 Sheet Alloy with Application to Axial Crushing," *Materials Science and Engineering: A*, Vol. 565, pp. 203-212, 2013.
4. Yoon, J., Lee, J., and Lee, J., "Enhancement of the Microstructure and Mechanical Properties in as-Forged Mg-8Al-0.5Zn Alloy using T5 Heat Treatment," *Materials Science and Engineering: A*, Vol. 586, pp. 306-312, 2013.
5. Yoon, J. and Park, S., "Forgeability Test of Extruded Mg-Sn-Al-Zn Alloys under Warm Forming Conditions," *Materials & Design*, Vol. 55, pp. 300-308, 2014.
6. Cazacu, O. and Barlat, F., "A Criterion for Description of Anisotropy and Yield Differential Effects in Pressure-Insensitive Metals," *International Journal of Plasticity*, Vol. 20, No. 11, pp. 2027-2045, 2004.
7. Cazacu, O., Plunkett, B., and Barlat, F., "Orthotropic Yield Criterion for Hexagonal Closed Packed Metals," *International Journal of Plasticity*, Vol. 22, No. 7, pp. 1171-1194, 2006.
8. Zhilyaev, A., Nurislamova, G., Kim, B.-K., Baró, M., Szpunar, J., and Langdon, T., "Experimental Parameters Influencing Grain Refinement and Microstructural Evolution during high-Pressure Torsion," *Acta Materialia*, Vol. 51, No. 3, pp. 753-765, 2003.
9. Iwahashi, Y., Wang, J., Horita, Z., Nemoto, M., and Langdon, T. G., "Principle of Equal-Channel Angular Pressing for the Processing of Ultra-Fine Grained Materials," *Scripta Materialia*, Vol. 35, No. 2, pp. 143-146, 1996.
10. Iwahashi, Y., Horita, Z., Nemoto, M., and Langdon, T. G., "The Process of Grain Refinement in Equal-Channel Angular Pressing," *Acta Materialia*, Vol. 46, No. 9, pp. 3317-3331, 1998.
11. Nakashima, K., Horita, Z., Nemoto, M., and Langdon, T. G., "Development of a Multi-Pass Facility for Equal-Channel Angular Pressing to high Total Strains," *Materials Science and Engineering: A*, Vol. 281, No. 1, pp. 82-87, 2000.
12. Kim, K. J., Yang, D. Y., and Yoon, J. W., "Microstructural Evolution and Its Effect on Mechanical Properties of Commercially Pure Aluminum Deformed by Ecae (Equal Channel Angular Extrusion) Via Routes A and C," *Materials Science and Engineering: A*, Vol. 527, No. 29, pp. 7927-7930, 2010.

13. Nie, K., Wu, K., Wang, X., Deng, K., Wu, Y., and Zheng, M., "Multidirectional Forging of Magnesium Matrix Composites: Effect on Microstructures and Tensile Properties," *Materials Science and Engineering: A*, Vol. 527, No. 27, pp. 7364-7368, 2010.
14. Chen, Q., Shu, D., Hu, C., Zhao, Z., and Yuan, B., "Grain Refinement in an As-Cast AZ61 Magnesium Alloy Processed by Multi-Axial Forging under the Multitemperature Processing Procedure," *Materials Science and Engineering: A*, Vol. 541, No. pp. 98-104, 2012.
15. Saito, Y., Utsunomiya, H., Tsuji, N., and Sakai, T., "Novel Ultra-high Straining Process for Bulk Materials—Development of the Accumulative Roll-Bonding (ARB) Process," *Acta Materialia*, Vol. 47, No. 2, pp. 579-583, 1999.
16. Kim, K. and Yoon, J., "Evolution of the Microstructure and Mechanical Properties of AZ61 Alloy Processed by Half Channel Angular Extrusion (HCAE), a Novel Severe Plastic Deformation Process," *Materials Science and Engineering: A*, Vol. 578, pp. 160-166, 2013.
17. Mabuchi, M., Ameyama, K., Iwasaki, H., and Higashi, K., "Low temperature Superplasticity of AZ91 Magnesium Alloy with Non-Equilibrium Grain Boundaries," *Acta Materialia*, Vol. 47, No. 7, pp. 2047-2057, 1999.
18. Yamashita, A., Horita, Z., and Langdon, T. G., "Improving the Mechanical Properties of Magnesium and a Magnesium Alloy through Severe Plastic Deformation," *Materials Science and Engineering: A*, Vol. 300, No. 1, pp. 142-147, 2001.
19. Watanabe, H., Mukai, T., Ishikawa, K., and Higashi, K., "Low Temperature Superplasticity of a Fine-Grained ZK60 Magnesium Alloy Processed by Equal-Channel-Angular Extrusion," *Scripta Materialia*, Vol. 46, No. 12, pp. 851-856, 2002.
20. Agnew, S. R., Mehrotra, P., Lillo, T. M., Stoica, G. M., and Liaw, P. K., "Texture Evolution of Five Wrought Magnesium Alloys during Route a Equal Channel Angular Extrusion: Experiments and Simulations," *Acta Materialia*, Vol. 53, No. 11, pp. 3135-3146, 2005.
21. Suwas, S., Gottstein, G., and Kumar, R., "Evolution of Crystallographic Texture during Equal Channel Angular Extrusion (ECAE) and Its Effects on Secondary Processing of Magnesium," *Materials Science and Engineering: A*, Vol. 471, No. 1, pp. 1-14, 2007.
22. Xia, K., Wang, J. T., Wu, X., Chen, G., and Gurvan, M., "Equal Channel Angular Pressing of Magnesium Alloy AZ31," *Materials Science and Engineering: A*, Vol. 410, pp. 324-327, 2005.
23. Tang, W. N., Chen, R. S., Zhou, J., and Han, E. H., "Effects of ECAE Temperature and Billet Orientation on the Microstructure, Texture Evolution and Mechanical Properties of a Mg-Zn-Y-Zr Alloy," *Materials Science and Engineering: A*, Vol. 499, No. 1, pp. 404-410, 2009.
24. Al-Maharbi, M., Karaman, I., Beyerlein, I. J., Foley, D., Hartwig, K. T., et al., "Microstructure, Crystallographic Texture, and Plastic Anisotropy Evolution in an Mg Alloy during Equal Channel Angular Extrusion Processing," *Materials Science and Engineering: A*, Vol. 528, No. 25, pp. 7616-7627, 2011.
25. Foley, D. C., Al-Maharbi, M., Hartwig, K. T., Karaman, I., Kecskes, L. J., and Mathaudhu, S. N., "Grain Refinement vs. Crystallographic Texture: Mechanical Anisotropy in a Magnesium Alloy," *Scripta Materialia*, Vol. 64, No. 2, pp. 193-196, 2011.
26. Yamashita, A., Horita, Z., and Langdon, T. G., "Improving the Mechanical Properties of Magnesium and a Magnesium Alloy through Severe Plastic Deformation," *Materials Science and Engineering: A*, Vol. 300, No. 1, pp. 142-147, 2001.
27. Lapovok, R., Thomson, P. F., Cottam, R., and Estrin, Y., "The Effect of Grain Refinement by Warm Equal Channel Angular Extrusion on Room Temperature Twinning in Magnesium Alloy ZK60," *Journal of Materials Science*, Vol. 40, No. 7, pp. 1699-1708, 2005.
28. Koike, J., Kobayashi, T., Mukai, T., Watanabe, H., Suzuki, M., et al., "The Activity of Non-Basal Slip Systems and Dynamic Recovery at Room Temperature in Fine-Grained AZ31B Magnesium Alloys," *Acta Materialia*, Vol. 51, No. 7, pp. 2055-2065, 2003.
29. Kim, W. J., An, C. W., Kim, Y. S., and Hong, S. I., "Mechanical Properties and Microstructures of an AZ61 Mg Alloy Produced by Equal Channel Angular Pressing," *Scripta Materialia*, Vol. 47, No. 1, pp. 39-44, 2002.